

CYCLOTRON MASER EMISSION OF AURORAL Z MODE RADIATION

R. G. Hewitt¹

Department of Astro-Geophysics, University of Colorado

D. B. Melrose

School of Physics, University of Sydney

G. A. Dulk²

Commonwealth Scientific and Industrial Research Organization
Division of Radiophysics

Abstract. Z mode radiation has been observed in the auroral zones where the plasma frequency ω_p is less than the electron cyclotron frequency Ω_e . We explore the possibility that this radiation is generated in the same way as the X mode radiation of the auroral kilometric radiation (AKR), i.e., by cyclotron maser emission driven by a loss cone distribution, specifically by electrons reflected at a lower height and propagating upward. We calculate the growth rate for the Z mode by using a method developed for the X mode and the O mode. We find: (1) Growth occurs in a small crescent-shaped region of $\omega - \theta$ space just outside a forbidden zone near $\theta = 90^\circ$ with ω between Ω_e and the upper hybrid frequency. (2) The temporal growth rate for the Z mode is less than that for the (unsuppressed) X mode but comparable with that of the O mode; for $\omega_p/\Omega_e > 0.3$ the X mode is suppressed and the growth of the Z mode and the O mode compete for the available free energy. Because of the low group speed of the Z mode its spatial growth rate is higher than that of the O mode, giving it an advantage. (3) The product of the spatial growth rate and the bandwidth of the growing waves for the Z mode is comparable with that for the (unsuppressed) X mode and is much greater than that of the O mode. (4) Although all growing Z mode waves have slightly upward directed wave normals ($\theta > 90^\circ$), most have downward directed rays, many at angles θ_g between 50° and 70° , and so can propagate toward regions where $\omega < \Omega_e$. We argue that these properties suggest that loss cone driven cyclotron emission may be the mechanism generating the observed auroral Z mode radiation.

1. Introduction

Broadband Z mode radiation has been detected in auroral cavities where the plasma frequency ω_p is appreciably less than the electron cyclotron frequency Ω_e . Calvert [1981] reported observations with the Hawkeye satellite, Benson [1982] with the ISIS 1 topside sounder and

¹On leave from School of Physics, University of Sydney.

²On leave from Department of Astro-Geophysics, University of Colorado.

Copyright 1983 by the American Geophysical Union.

Paper number 3A1483.
0148-0227/83/003A-1483\$05.00

Gurnett et al. [1983] with the polar orbiting DE-1 spacecraft. It seems that Z mode radiation is a common feature of the auroral zones and that it had not been identified earlier because it is difficult to distinguish from auroral hiss under conditions when $\Omega_e > \omega_p$. The frequency band in which the Z mode can exist overlaps with the upper end of the whistler band and hence of auroral hiss. There is not a strong correlation between the observed Z mode radiation and either auroral hiss or auroral kilometric radiation (AKR), although the correlation is somewhat better with hiss. The intensity of the Z mode radiation is about 10^{-3} of that of the simultaneously detected AKR [Gurnett et al., 1983].

By analogy either to the generation of hiss or to the generation of AKR there are two obvious possibilities for the generation of Z mode radiation. Hiss is thought to be generated through amplified Cerenkov emission by downgoing electrons [Swift and Kan, 1975; Maggs, 1976; Yamamoto, 1979; Melrose and White, 1980; Lotko and Maggs, 1981]. Cerenkov emission requires a large refractive index, and the Z mode has a resonance (i.e., an infinite refractive index) at $\omega = \omega_+(\theta)$ with $\omega_+(\theta) > \Omega_e > \omega_p$. The observed Z mode radiation would then be attributed to downward propagating radiation initially generated at $\omega > \Omega_e$. Gurnett et al. [1983] have commented briefly on this mechanism. Here we discuss the other, a mechanism analogous to that for AKR.

Following the suggestion by Wu and Lee [1979] it is now widely accepted that AKR is generated through a loss cone driven cyclotron maser emission by reflected upgoing electrons [Omidi and Gurnett, 1982; Melrose et al., 1982; Wu et al., 1982; Dusenbery and Lyons, 1982]. Hewitt et al. [1982] explored the properties of this maser, including emission in both magnetoionic modes above their cutoff frequencies at harmonics $s = 1, 2,$ and 3 . They performed detailed numerical calculations for an idealized but fairly realistic loss cone distribution function, and developed a semiquantitative theory including all these effects. The properties of the waves were assumed to be determined by magnetoionic theory, i.e., the dispersion is due solely to a relatively dense cold background plasma.

More recently, Hewitt and Melrose [1983] extended the analysis to include emission near the cutoff frequencies. In the present paper we report a further extension to include cyclotron maser emission in the Z mode. We find that the Z mode can grow in a narrow, crescent-shaped band in $\omega - \theta$ space (θ is the wave normal angle

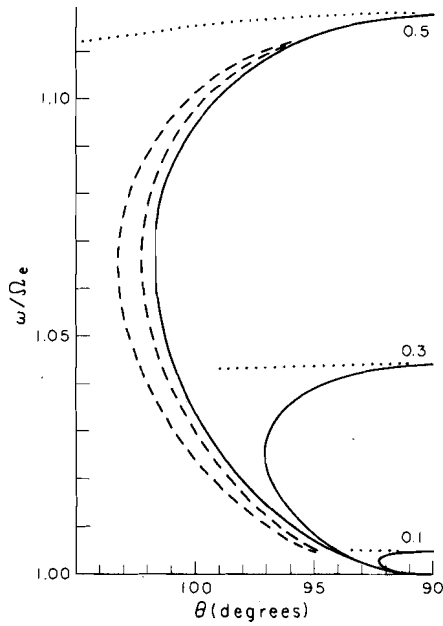


Fig. 1. The curves for $V = 0$ (solid lines) and $\omega = \omega_+(\theta)$ (dotted lines) are plotted for various values of ω_p/Ω_e as indicated by the labels on the curves. Resonance between the electrons and the waves is possible to the left of the $V = 0$ curve and below the $\omega = \omega_+(\theta)$ curve. The dashed crescents denote the half-maximum growth points (at fixed θ) for $\omega_p/\Omega_e = 0.5$.

relative to the downward direction parallel to the magnetic field) at a frequency above Ω_e and below the resonant frequency ω_+ . The radiation has its wave normal directed nearly perpendicular to the magnetic field and slightly upward ($\theta > 90^\circ$); however, it can be downgoing in the sense that the group velocity is directed downward. In other words, if θ_g is the angle between the group velocity and the downward direction parallel to the magnetic field, then we can have $\theta_g < 90^\circ$.

In section 2 we discuss the kinematics for cyclotron emission in the Z mode, and in section 3 we present our numerical results. The group properties, concentrating on the conditions for $\theta_g < 90^\circ$ with $\theta > 90^\circ$, are discussed in section 4, and the application to the observations is discussed in section 5.

2. Kinematics

The cyclotron resonance condition for the s th harmonic

$$\omega - s\Omega_e/\gamma - k_{\parallel}v_{\parallel} = 0 \quad (1)$$

with $\gamma = (1 - v_{\parallel}^2/c^2 - v_{\perp}^2/c^2)^{-1/2}$ may be represented by an ellipse in velocity (v_{\parallel}, v_{\perp}) space [Hewitt et al., 1981; Omid and Gurnett, 1982; Melrose et al., 1982]. Here the subscript parallel and perpendicular denotes components parallel and perpendicular to the (downward) magnetic field. Let $(v_{\parallel}, v_{\perp}) = (v_c, 0)$ denote the center of the ellipse and V denote its semimajor axis (parallel to the v_{\perp} axis).

Then we have

$$\frac{v_c}{c} = \frac{\omega k_{\parallel} c}{k_{\parallel}^2 c^2 + s^2 \Omega_e^2} \quad (2)$$

$$\frac{V^2}{c^2} = \frac{k_{\parallel}^2 c^2 + s^2 \Omega_e^2 - \omega^2}{k_{\parallel}^2 c^2 + s^2 \Omega_e^2} \quad (3)$$

Here we shall be concerned only with fundamental emission ($s = 1$) in the Z mode. The Z mode, which is the lower frequency branch of the X mode, exists between the cutoff frequency at

$$\omega_{xL} = -\frac{1}{2}\Omega_e + \frac{1}{2}[\Omega_e^2 + 4\omega_p^2]^{1/2} \quad (4)$$

and the resonance at $\omega_+(\theta)$,

$$\omega_+^2(\theta) = \frac{1}{2}(\omega_p^2 + \Omega_e^2) + \frac{1}{2}[(\omega_p^2 + \Omega_e^2)^2 - 4\omega_p^2 \Omega_e^2 \cos^2 \theta]^{1/2} \quad (5)$$

Note that the resonance frequency ω_+ is equal to the upper hybrid frequency ω_{UH} at $\theta = 90^\circ$ and is close to but slightly less than ω_{UH} for other relevant values of θ . The specific formulas we use for the refractive index n of the Z mode, and hence for $k_{\parallel} = n(\omega/c)\cos \theta$, are written down in the appendix.

The main kinematic restrictions arise from the coupled requirements that V^2 be positive and that $k_{\parallel} = n(\omega/c)\cos \theta$ in (3) satisfying the dispersion relation for Z mode waves. For $\omega_p \ll \Omega_e$ the refractive index curve for the Z mode plotted as a function of ω for fixed θ rises rapidly to $n \approx 1$ just above the cutoff frequency, remains roughly constant for $\omega_{xL} < \omega < \Omega_e$ and then rises rapidly to infinity at $\omega = \omega_+(\theta)$. For $s = 1$ the requirement $V^2 > 0$ is automatically satisfied for $\omega < \Omega_e$, and for $\Omega_e < \omega < \omega_+(\theta)$ a small region of $\omega - \theta$ space near $\theta = 90^\circ$ is excluded, as illustrated in Figure 1. The existence of this excluded region can be inferred by plotting the Doppler condition (3) with $V = 0$ in terms of n^2 as a function of ω for fixed θ . This "Doppler curve" rises rapidly from $n^2 = 0$ at $\omega = \Omega_e$ and tends to $n^2 = 1/\cos^2 \theta$ for arbitrarily large ω . This approach has been used by Ellis [1962], Fung and Yip [1966], and Hewitt and Melrose [1983] in connection with other modes. For $\Omega_e > \omega_{xL}$, i.e., $\omega_p/\Omega_e < \sqrt{2}$, the Doppler curve and the refractive index curve intersect twice or not at all, and for $\omega_p/\Omega_e > \sqrt{2}$ they intersect once or three times. We are interested only in the case $\omega_p/\Omega_e < \sqrt{2}$ and the excluded region in $\omega - \theta$ space corresponds to those values of θ for which two intersections occur and of ω between the intersection frequencies.

Growth of the Z mode is kinematically possible for $\omega_{xL} < \omega < \omega_+(\theta)$; however, for $\omega_{xL} < \omega < \Omega_e$ growth does not occur for the loss cone distributions we have considered. We find growth only for those values of ω and θ that correspond to resonant ellipses totally or almost totally inside the loss cone. This condition gives a second kinematic restriction for amplification to be effective. (Other types of distributions with an alternative source of free energy, e.g., those with trapped electrons, can cause growth for $\omega < \Omega_e$.) A related kinematic restriction for a one-sided loss cone distribution is that the

ellipse must be on the same side of the v_{\perp} axis as the loss cone. This requires $\alpha > 90^\circ$ for $\alpha_0 > 90^\circ$. Thus, for an upward directed loss cone only upward directed waves can grow.

3. Detailed Results

Our method of calculation has been described by Hewitt et al. [1982]. Here we choose the same loss cone distribution function for the energetic electrons as in that work; specifically, in terms of the speed v and pitch angle α ,

$$f(v, \alpha) = \frac{n_H g_N(\alpha)}{(2\pi v^2)^{3/2}} \exp\left[-\frac{v^2}{2v_e^2}\right] \quad (6)$$

with

$$g_N(\alpha) = \begin{cases} a_N & \alpha \leq \alpha_0 \\ a_N \left[\sin\left[\frac{1}{2}\pi(\pi - \alpha)/(\pi - \alpha_0)\right] \right]^N & \alpha > \alpha_0 \end{cases} \quad (7)$$

where n_H is the number density of the energetic electron component, assumed to be the Maxwellian with $v_e = (KT_e/m_e)^{1/2}$ outside of the loss cone, i.e., for pitch angles $\alpha \leq \alpha_0$. We may approximate the normalization constant a_N by unity [cf. Hewitt et al., 1982]. Here all our calculations are for $N = 6$. (The specific choice of the "steepness parameter" N affects the growth rate for the Z mode in much the same way as it does for the X mode and the O mode: Compare Figure 3 of Hewitt et al. [1982].) The other numerical values are the same as those used in the work of Hewitt et al. [1982], i.e., $\alpha_0 = 150^\circ$ and $T_e = 10^6$ K so that $KT_e \approx 10$ keV; n_H and Ω_e are held fixed and the number density of the cold back-

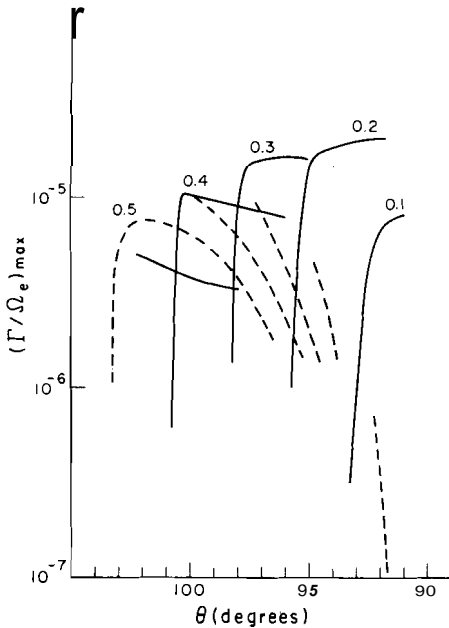


Fig. 2. The normalized maximum temporal growth rates $(\Gamma/\Omega_e)_{\max}$ are plotted as a function of θ for the indicated values of ω_p/Ω_e . For each horn of the crescent-shaped regions in Figure 1 there is a growth band, an upper band (solid curve), and a lower band (dashed curve).

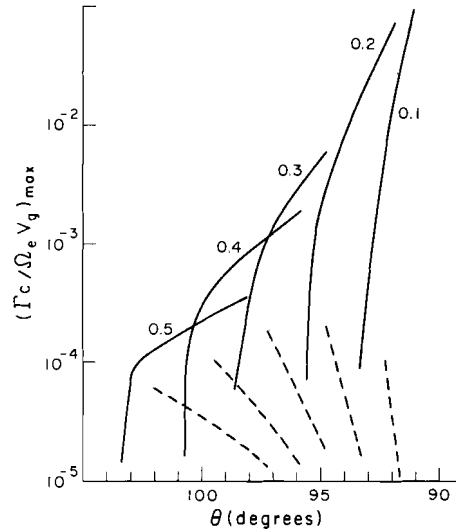


Fig. 3. As in Figure 2 but for the normalized maximum spatial growth rate $(\Gamma_c/\Omega_e v_g)_{\max}$.

ground electrons n_C (and hence ω_p/Ω_e) is varied. The growth rate Γ scales as Ω_e so that Γ/Ω_e is a function of the ratios n_H/n_C and ω_p/Ω_e and not of ω_p and Ω_e separately. The parameters are chosen such that $n_H/n_C = 10^{-2}$ when $\omega_p/\Omega_e = 0.1$.

Figure 1 shows, for various values of ω_p/Ω_e , the curves defining the upper frequency limit $\omega_+(\theta)$ of the Z mode (dotted) and the curves defining the values where the resonance ellipse vanishes (solid). The region of growth consists of a narrow crescent in the $\omega - \theta$ plane near the $V = 0$ curve. For a particular value of θ close to 90° there are in general two ranges of ω where growth occurs. We refer to these, the two horns of the crescent, as the two growth bands. As θ increases above 90° the two bands approach each other, overlap, and then disappear. Thus growth is possible only for $90^\circ < \theta < \theta_{\max}$ with θ_{\max} a function of ω_p/Ω_e (empirically, $|\cos \theta_{\max}| \approx \omega_p/2\Omega_e$). The half-maximum growth points of the two bands for fixed θ and $\omega_p/\Omega_e = 0.5$ are indicated by dashed lines in Figure 1.

We have searched these two bands to find the maximum temporal growth rate (as a function of ω) for each choice of θ . These maximum growth rates are plotted in Figure 2. The upper band has the larger growth rate for $\omega_p/\Omega_e < 0.4$, and for $\omega_p/\Omega_e > 0.5$ the lower band dominates. Note that the growth rates are directly proportional to n_H and higher values can be achieved for denser energetic electron distributions. There is, however, an implicit limitation on the value of n_H/n_C for our neglect of the effect of the energetic electrons on the dispersive properties to remain valid.

In Figure 3 we plot the maximum spatial growth rate for the same parameters as in Figure 2. The smaller group speed v_g in the upper band tends to favor its spatial growth over that of the lower band. In Figure 4 we plot the difference between the two frequencies where the spatial growth rate falls to half its maximum value for each band; we call this the bandwidth $\Delta\omega$ of the growing waves. Similar calculations for the X mode and the O mode have been presented by Hewitt

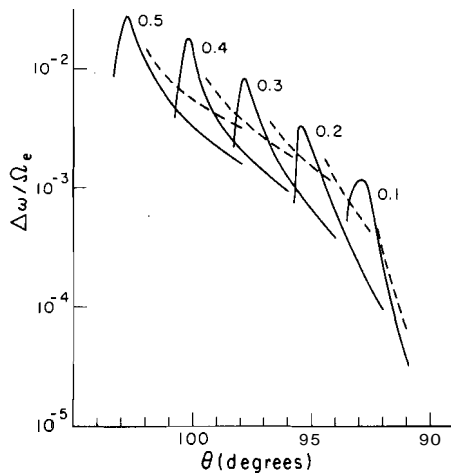


Fig. 4. The normalized bandwidth $\Delta\omega/\Omega_e$ of the growing waves (as defined in the text) is plotted as a function of θ for the indicated values of ω_p/Ω_e . The solid and dashed curves are for the upper and lower bands, respectively.

et al. [1982] and Hewitt and Melrose [1983].

Growth may be limited either by the temporal growth rate and saturation (as is usually assumed) or by geometrical considerations, e.g., the width of the flux tube in which the unstable electrons are confined. The effectiveness of growth depends on the magnitude of the spatial growth rate and the distance over which growth is possible, and this growth path is also limited by changes in the magnetic field strength along the ray path. Specifically, growth ceases when Ω_e has changed by an amount equal to the bandwidth of the growing waves. Provided the secant of the angle between the ray direction and grad B does not change appreciably, a measure of the effectiveness of amplification is the product of the spatial growth rate times the bandwidth of the growing waves [Hewitt and Melrose, 1983]. We plot this product in Figure 5, where it is seen that growth in the upper band is favored over that in the lower band. The upper band is favored mainly because of the lower group speeds than for the lower band.

Comparison With the X mode and the O mode

Comparing the temporal growth rates for the X mode and the O mode [Hewitt et al., 1982; Hewitt and Melrose, 1983; Dulk and Melrose, 1983] with that of the Z mode, we find that the X mode is the fastest growing mode, by a factor > 10 for $\omega_p/\Omega_e < 0.3$. The X mode is strongly suppressed for $\omega_p/\Omega_e \geq 0.3$. The maximum temporal growth rates for the O mode and Z mode differ by no more than a factor of 2 for $0.1 < \omega_p/\Omega_e < 1.0$. The growth of the Z mode is relatively more favored when we consider the spatial growth rate in Figure 3 and, especially, the product plotted in Figure 5. The values for the Z mode are comparable with those of the X mode and much greater than those for the O mode. This is due largely to the small group speed for the Z mode in the upper growth band.

4. The Group Velocity

A surprising feature of the Z mode radiation in the range where growth occurs is that although the wave vectors are directed upward ($\theta > 90^\circ$) the group velocity is usually directed downward (ray angle $\theta_g < 90^\circ$). In Figure 6 we plot θ_g versus θ for the cases considered in Figures 2 to 5. In each case the downward direction of the rays is most noticeable in the upper band, especially where θ is closest to 90° , corresponding to frequencies relatively close to the resonant frequency $\omega_+(\theta)$. Comparison of Figure 2 or 5 with 6 shows that, for $\omega_p/\Omega_e = 0.2$ to 0.4 , the ray angle θ_g is in the range $\approx 50^\circ$ to 70° when the growth rate is near its maximum.

In the appendix we derive an expression for the group angle θ_g for $\cos^2 \theta \ll 1$ and for $\omega = \Omega_e > \omega_p$. For $\omega^2 - \Omega_e^2 \gg \omega_p^2 \cos^2 \theta$ the result (A15) simplifies to

$$\cot \theta_g = \frac{\omega^2 - \Omega_e^2}{\omega^2 - \omega_{UH}^2} \cos \theta \tag{8}$$

where $\omega_{UH} = (\omega_p^2 + \Omega_e^2)^{1/2}$ is the upper hybrid frequency. The frequency range for wave growth is

$$\Omega_e^2 < \omega^2 < \omega_+^2(\theta) \leq \omega_{UH}^2 \tag{9}$$

so that $\cot \theta_g$ has the opposite sign to $\cos \theta$. In the upper growth band the difference $\Omega_e^2 + \omega_p^2 - \omega^2$ is smaller than $\omega^2 - \Omega_e^2$ and (8) implies $|\cot \theta_g| > |\cos \theta|$. This case corresponds to the solid curves in Figure 6.

We have also explored the relation between θ and θ_g using Poverlein's construction, and we comment on this here for those readers who are familiar with this technique. An example of the

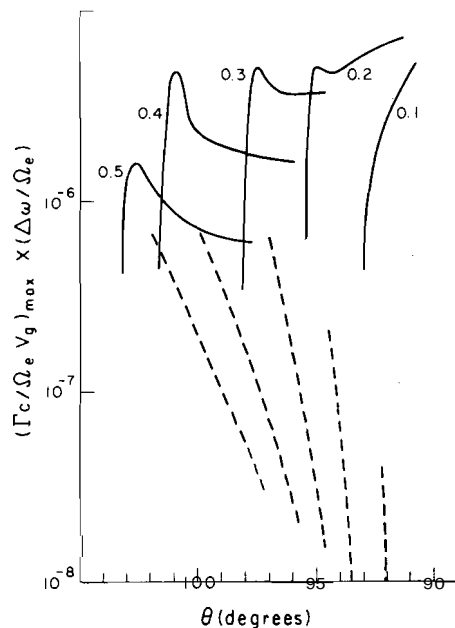


Fig. 5. The product of the maximum spatial growth rate (Figure 3) and the bandwidth of the growing waves (Figure 5) is plotted as a function of θ for the indicated values of ω_p/Ω_e .

I
P
u
t
t
a

polar plot of $n(\omega, \theta)$ for the Z mode is given in Figure 13.26 of Budden [1961]. For $X < 1$ (cf. his curve for $X = 0.8$) and for θ close to 90° the curves of $n(\omega, \theta)$ are essentially concave (i.e., $\partial^2 n / \partial \theta^2 > 0$) with their closest point to the origin being at $\theta = 90^\circ$. For $\omega_p / \Omega_e = 0.5$ say, the analogous curves vary from weakly concave (with a small weakly convex section near $\theta = 90^\circ$) at $n \geq 1$ for $\omega / \Omega_e \approx 1.01$ to strongly concave with closest point at $n \geq 2$ for $\omega / \Omega_e \geq 1.1$. Granted this concave shape near $\theta = 90^\circ$ for upper band frequencies it is obvious that for $\theta \geq 90^\circ$ the group velocity is directed downward ($\theta_g < 90^\circ$). In the curve we have drawn in Figure 6 for $\omega_p / \Omega_e = 0.5$ the strongly downward directed upper band rays correspond to refractive indices between about 2 and 3.

We conclude that although the wave normals of the waves in the upper growth band are directed nearly perpendicular to but slightly up the magnetic field, the corresponding rays are directed down the magnetic field at a moderately large angle to it.

5. Discussion

The main results of our investigation of loss cone driven maser emission for the Z mode are given below.

1. Waves in the Z mode grow in a crescent-shaped region in $\omega - \theta$ space with ω in the range $\Omega_e < \omega < \omega_+(\theta)$, where $\omega_+(\theta)$ is the resonant frequency, and with $\theta = 90^\circ$ reaching its maximum value near the middle of this frequency range.

2. The magnitude of the temporal growth rate for the Z mode is smaller than that of the fundamental X mode for $\omega_p / \Omega_e < 0.3$ and comparable to that of the fundamental O mode; for $\omega_p / \Omega_e > 0.3$ the fundamental X mode becomes strongly suppressed.

3. The number of e folding growths, estimated from the product of the spatial growth rate and the bandwidth of the growing waves, indicates that growth of the Z mode can be more favorable than estimates based only on the temporal growth rate would suggest.

4. Despite the wave normals being directed slightly upward ($\theta > 90^\circ$) the ray directions are usually downward ($\theta_g < 90^\circ$). This effect is most pronounced for growth in the upper frequency band, where θ_g can be directed quite strongly downward, e.g., $\theta_g = 50^\circ$ to 70° .

These properties seem favorable for the interpretation of the observed Z mode radiation. We would expect the Z mode radiation to be generated, perhaps along with O mode radiation, in regions with $\omega_p / \Omega_e > 0.3$. (It is possible in principle for it to be generated in regions with $\omega_p / \Omega_e < 0.3$, but then it must tap a source of free energy that is not available to the faster growing X mode radiation.)

The fact that the initial direction of energy propagation is downward, despite the wave normal being directed upward, is of major consequence. It implies that the wave energy does not propagate directly into the resonance at $\omega = \omega_+(\theta)$, where it would be absorbed by thermal electrons. An important question is how the energy continues to propagate. Gurnett et al. [1983] commented on the ray propagation for

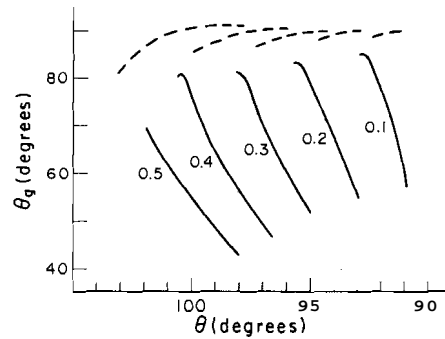


Fig. 6. The group angle θ_g is plotted as a function of the wave normal angle θ for the curves in Figure 2. Note that in the upper frequency band (solid curves) we have $\theta_g < 90^\circ$ for $\theta > 90^\circ$.

the Z mode by using Poeverlein's construction and assuming a source at $\omega < \Omega_e$. They argued that the radiation can propagate large distances, with refraction causing the rays to become nearly horizontal just below the cyclotron layer $\omega = \Omega_e$.

In the cyclotron maser mechanism the radiation is generated at $\omega > \Omega_e$; the peculiar wave and ray properties that lead to $\theta_g < 90^\circ$ for $\theta > 90^\circ$ in this regime were not considered by Gurnett et al. [1983]. It is possible for some of the rays that are initially propagating downward to cross the cyclotron layer to the location where $\omega < \Omega_e$ and the Z mode waves are observed. For this to happen the group velocity at the cyclotron layer where \mathbf{v}_g is perpendicular to \mathbf{B} must satisfy $\mathbf{v}_g \cdot \text{grad } B < 0$. The subsequent propagation of the rays could then be as described by Gurnett et al. [1983]; however, detailed ray tracing is required to determine just how the Z mode rays actually propagate, and we have not yet attempted such calculations. From (8) we see that, as the cyclotron layer is approached from above, the rays tend to $\theta_g = 90^\circ$, and from (A15) we see that this occurs somewhat above the cyclotron layer. For the rays to enter the region $\omega < \Omega_e$, refraction must cause $\cos \theta$ to change sign near the layer where $\cos \theta_g$ is close to zero. In other words, the point $\cos \theta_g = 0$ must be a point of inflection rather than of reflection.

In conclusion, our results suggest that loss cone driven cyclotron maser emission by upgoing electrons, closely analogous to AKR, may be the mechanism generating the observed Z mode radiation. The lack of a strong correlation between the Z mode radiation and AKR is not surprising on this hypothesis: the ray paths for the X mode and the Z mode are markedly different, with the former directed upward and the latter downward. In addition, we expect the generation of the Z mode to be favored only in regions with $\omega_p / \Omega_e > 0.3$, i.e., where the X mode radiation is suppressed. An important point that we have not explored in detail is what fraction of the radiation generated crosses the cyclotron layer. If this is large, then the argument in favor of the loss cone driven cyclotron maser as the source of the observed Z mode radiation is a strong one: the spatial growth rates are quite

large in comparison with those for the X mode [Hewitt and Melrose, 1983], and there seems little doubt that Z mode radiation should be generated under conditions that differ only slightly from those for the generation of X mode radiation in AKR.

Appendix

The Group Angle for the Z mode for $\omega \approx \Omega_e > \omega_p$

Following Melrose [1980, p. 258 and 261], the group velocity for a magnetoionic wave is of the form

$$\mathbf{v}_g = \frac{c}{\partial(\omega n)} (\underline{\kappa} - \frac{KT}{1+T^2} \underline{t}) \quad (\text{A1})$$

where the polarization vector is written

$$\underline{e} = \frac{K\underline{\kappa} + T\underline{t} + i\underline{a}}{(K^2 + T^2 + 1)^{1/2}} \quad (\text{A2})$$

with $\underline{\kappa}$ along \underline{k} , \underline{B} along the Z axis, and

$$\begin{aligned} \underline{\kappa} &= (\sin \theta, 0, \cos \theta) \\ \underline{t} &= (\cos \theta, 0, -\sin \theta) \\ \underline{a} &= (0, 1, 0) \end{aligned} \quad (\text{A3})$$

The axial ratio T satisfies

$$T^2 + \frac{Y \sin^2 \theta}{(1-X) \cos \theta} T - 1 = 0 \quad (\text{A4})$$

where $X = \omega_p^2/\omega^2$ and $Y = \Omega_e/\omega$ are the magnetoionic parameters. The relevant solution of (A4) for the Z mode is

$$T = \frac{2Y(1-X) \cos \theta}{Y^2 \sin^2 \theta + 2\Delta} \quad (\text{A5})$$

$$\Delta^2 = \frac{1}{4} Y^4 \sin^4 \theta + Y^2 (1-X)^2 \cos^2 \theta \quad (\text{A6})$$

and K is given by

$$K = \frac{XY \sin \theta}{1-X} \frac{T}{T - Y \cos \theta} = \frac{XY \sin \theta (1 + Y T \cos \theta)}{1 - X - Y^2 + XY^2 \cos^2 \theta} \quad (\text{A7})$$

The refractive index, which we require for our numerical calculations, is given by

$$n^2 = 1 - \frac{KT}{T - Y \cos \theta} = 1 - \frac{X(1-X)(1 + Y T \cos \theta)}{1 - X - Y^2 + XY^2 \cos^2 \theta} \quad (\text{A8})$$

The Z mode wave resonant frequency (5) is the higher frequency solution of

$$1 - X - Y^2 + XY^2 \cos^2 \theta = 0 \quad (\text{A9})$$

where the refractive index is infinite and the waves are longitudinal ($K = \infty$ for finite T).

The group angle θ_g is defined by

$$\mathbf{v}_g = v_g (\sin \theta_g, 0, \cos \theta_g) \quad (\text{A10})$$

Then (A1) with (A3) gives

$$\tan \theta_g = \frac{\tan \theta + \tan \theta_0}{1 - \tan \theta \tan \theta_0} \quad (\text{A11})$$

i.e., $\theta_g = \theta + \theta_0$, with

$$\tan \theta_0 = - \frac{KT}{1 + T^2} \quad (\text{A12})$$

We assume that Y and $1-X$ are of order unity and much greater than $\cos^2 \theta$. Then we have

$$T = \frac{(1-X) \cos \theta}{Y \sin^2 \theta} \quad (\text{A13})$$

and

$$\tan \theta_0 = - \frac{X(1-X) \cot \theta}{1 - X - Y^2 + XY^2 \cos^2 \theta} \quad (\text{A14})$$

with $\cot \theta = \cos \theta$. Substitution of (A14) into (A11) gives

$$\begin{aligned} \cot \theta_g &= \frac{1 - X^2 - Y^2 + XY^2 \cos^2 \theta}{1 - X - Y^2} \cot \theta \\ &= \frac{\omega^2 - \Omega_e^2 - (\omega_p^2/\omega^2)(\omega_p^2 - \Omega_e^2 \cos^2 \theta)}{\omega^2 - (\Omega_e^2 + \omega_p^2)} \cot \theta \end{aligned} \quad (\text{A15})$$

Acknowledgments. Part of this work was supported by NASA's Solar Terrestrial Theory and Solar Heliospheric Physics Programs under grants NAGW-91 and NSG-7287 to the University of Colorado. We wish to thank R. Benson for helpful comments on the original manuscript.

The Editor thanks W. Calvert and C. S. Wu for their assistance in evaluating this paper.

References

- Benson, R. F., Harmonic auroral kilometric radiation of natural origin, *Geophys. Res. Lett.*, **9**, 1120, 1982.
- Budden, K. G., *Radio Waves in the Ionosphere*, Cambridge University Press, New York, 1961.
- Calvert, W., The auroral plasma cavity, *Geophys. Res. Lett.*, **8**, 919, 1981.
- Dulk, G. A., and D. B. Melrose, Electron-cyclotron masers at decimeter wavelengths and possible analogous mechanisms at meter wavelengths, in *Solar Noise Storms*, edited by A. O. Benz and P. Zlobec, p. 219, Osservatorio Astronomico di Trieste, Trieste, 1983.
- Dusenbery, P. B., and L. R. Lyons, General concepts on the generation of auroral kilometric radiation, *J. Geophys. Res.*, **87**, 7476, 1982.
- Ellis, G. R. A., Cyclotron radiation from Jupiter, *Aust. J. Phys.*, **15**, 344, 1962.
- Fung, P. C. W., and W. K. Yip, Cyclotron radiation from electron streams as the origin of solar type I noise storms, *Aust. J. Phys.*, **19**, 759, 1966.
- Gurnett, D. A., S. D. Shawhan, and R. R. Shaw, Auroral hiss, Z mode radiation and auroral kilometric radiation in the polar magnetosphere: DE-1 observations, *J. Geophys. Res.*, **88**, 329, 1983.
- Hewitt, R. G., and D. B. Melrose, Electron cyclotron maser emission near the cutoff frequencies, *Aust. J. Phys.*, in press, 1983.
- Hewitt, R. G., D. B. Melrose, and K. G. Rönmark, A cyclotron theory for the beaming pattern of

Jupiter's decametric radio emission, Proc. Astron. Soc. Aust., **4**, 221, 1981.

Hewitt, R. G., D. B. Melrose, and K. G. Rönmark, The loss-cone driven electron-cyclotron maser; Aust. J. Phys., **35**, 447, 1982.

Lotko, W., and J. E. Maggs, Amplification of electrostatic noise in cyclotron resonance with an adiabatic auroral beam, J. Geophys. Res., **86**, 3449, 1981.

Maggs, J. E., Coherent generation of VLF hiss, J. Geophys. Res., **81**, 1707, 1976.

Melrose, D. B., Plasma Astrophysics, Vol. 11, Gordon and Breach, New York, 1980.

Melrose, D. B., and S. M. White, Amplified Cerenkov emission of auroral hiss: Limitations implied by quasi-linear theory, J. Geophys. Res., **85**, 3442, 1980.

Melrose, D. B., K. G. Rönmark, and R. G. Hewitt, Terrestrial kilometric radiation: The cyclotron theory, J. Geophys. Res., **87**, 5140, 1982.

Omid, N., and D. A. Gurnett, Growth rate calculations of auroral kilometric radiation using the relativistic resonance condition, J. Geophys. Res., **87**, 2377, 1982.

Swift, D. W., and J. R. Kan, A theory of auroral

hiss and implications on the origin of auroral electrons, J. Geophys. Res., **80**, 985, 1975.

Wu, C. S., and L. C. Lee, A theory of terrestrial kilometric radiation, Astrophys. J., **230**, 621, 1979.

Wu, C. S., H. K. Wong, D. J. Gorney, and L. C. Lee, Generation of auroral kilometric radiation, J. Geophys. Res., **87**, 4476, 1982.

Yamamoto, T., On the amplification of VLF hiss, Planet. Space. Sci., **27**, 273, 1979.

G. A. Dulk, Commonwealth Scientific and Industrial Research Organization, Division of Radiophysics, P. O. Box 76, Epping, New South Wales 2121, Australia.

R. G. Hewitt, Department of Astro-Geophysics, University of Colorado, Boulder, CO 80309.

D. B. Melrose, School of Physics, University of Sydney, Sydney, New South Wales 2006, Australia.

(Received June 8, 1983;
revised August 29, 1983;
accepted September 9, 1983.)